Biochimica et Biophysica Acta, 731 (1983) 346–353
Elsevier

BBA 71686

OSMOTIC DEFORMATION OF RED BLOOD CELL GHOSTS INDUCED BY CARBOHYDRATES

TAIHYUN CHANG, PHILIP B. SHARPLESS *, DEBORAH A. DAVENPORT *, MICHAEL B. RADUNSKY and HYUK YU **

Department of Chemistry, University of Wisconsin-Madison, Madison, WI 53706 (U.S.A.)

(Received January 3rd, 1983)

Key words: Osmotic deformation; Erythrocyte ghost; Light scattering; Carbohydrate

The osmotic response of bovine red blood cell ghosts to a series of sugars is studied by light scattering. The sealed and right-side-out ghosts are prepared by the procedure of Steck and Kant (Steck, T.L. and Kant, J.A. (1974) Methods Enzymol. 31, 172–180), swollen in a hypotonic phosphate-buffered saline solution and their size and shape determined by elastic and quasielastic light scattering. Different carbohydrates are then added to the suspending medium in order to examine the osmotic responses, and the osmotic deformation of ghosts is shown to be spherically symmetric. Having thus established the deformation behavior, we then rank the osmotic activity of a carbohydrate relative to a standard, i.e., raffinose. It is found that the osmotic response of the ghosts to sucrose is about the same as that to raffinose, and the response to the smaller carbohydrates simply follows the number of carbons in various sugars; glucose and fractose are about 1.7 times less effective than raffinose, and pentaerythritol and *meso*-erythritol are 2.3 times less effective. Glyceraldehyde, which is 3.6 times less effective than raffinose, is the least effective sugar analog among those that we have tested.

Introduction

In the past several decades, the red blood cells have been the subject of extensive research, especially as the model case for biological membrane studies [1,2]. The system is well suited for membrane research because it is easily isolated by osmotic lysis to yield a very simple hemoglobin-free system, i.e., red blood cell ghost. Moreover, ghost membranes have been shown to preserve the same sidedness [3,4], the lipid composition [5,6], as well as the majority of the proteins [3,5] and the permeability toward small solute [4], including the active transport system [6,7], as the native red blood cell. Thus, the permeability studies of the ghost membranes have about the same significance as those on the intact red blood cell.

In this paper we present a straightforward method to monitor the osmotic response of red blood cell membranes by determining the shape and size of ghost vesicles with light scattering. Since the ghost membranes are known to respond to the osmotic gradient across the bilayer, the vesicles behave like osmometers and the extent of the gradient's deformation relative to the hypotonic state is directly related to the effective osmolarity of a given solute that is used to vary the osmotic gradient. Such a scheme to measure the effective osmolarity and thus to probe the permeability of a membrane system toward a variety of solutes has been used earlier with bovine disk membranes of retinal rod outer segment [8]. More recently, Amis and Yu [9] have performed a light-scattering study with red blood cell ghosts prepared by the procedure of Dodge et al. [5],

* Present address: Medical School, University of Wisconsin, Madison, WI 53706, U.S.A.
** To whom correspondence should be addressed.

which showed no osmotic response due to the expected leakiness of the resulting ghosts [4].

In this work, we prepare the ghost membranes by the procedure of Steck and Kant [4] which is known to produce the sealed and right-side-out vesicles, and show unambiguously the osmotic responses of the membrane vesicles.

Materials and Methods

Materials. Fresh cow blood was received in acid/ citrate/ dextrose or citrate/ phosphate/ dextrose solution and kept at 4°C. While both anticoagulants preserve the blood for 3 weeks without affecting the osmotic response of the prepared ghosts, the citrate/ phosphate/ dextrose solution was slightly better in terms of its retention of osmotic response.

Ghost membranes were prepared by the procedure of Steck and Kant [4] using 20 mosM phosphate buffer (pH 8) for the hemolysis followed by 1 h incubation with 320 mosM (isotonic) phosphate-buffered saline solution, pH 8, at 37°C. During this period the membranes are known to reseal and the sealed ghosts were then washed three times with cold phosphate-buffered saline at 4°C. The ghosts were stored in a small volume of isotonic phosphate-buffered saline at 4°C, and they remained good for about a week.

Elastic light scattering. Elastic light-scattering measurements were performed with the same instrument as was reported earlier [9], with several minor modifications. For some early measurements, an Ar ion laser (Lexel Model 75-.2) was used as the light source. A He-Ne laser (Aerotech, 5 mW), however, has been used in the latter part of the study because these measurements did not require an intense green light source. Despite the resulting scattering profile giving rise to a smaller number of structural features because of the longer wavelength of the incident source (632.8 nm), it is still possible to extract a sufficient number of modulation peaks [10] which allows us to calculate quite precisely the size of the vesicles. For more facile data acquisition and better signal to noise ratio, a microcomputer (Apple II) controlled stepper motor was installed to drive the goniometer and the photodiode was replaced by a photomultiplier tube (Hamamatsu, R928). A fiber optics (Edmund Scientific Co., 1/16 inch diameter) was used to guide the scattered light from the exit pinhole to the photocathode of the photomultiplier tube.

For the light scattering solutions, a filtered (10 μm Nucleopore) aliquot of the ghost stock suspension was added to a volume of prefiltered (0.45 μm, Gelman) suspending medium such that the final suspension had a well-defined concentration of phosphate-buffered saline. The scattered intensity was measured from 7.0° to 24.6° at 0.2° increments.

In the osmotic deformation study, the osmolarity of the starting suspension was made to 200 mosM phosphate-buffered saline in order to ensure full expansion of the ghost vesicles since this has been shown to be sufficiently hypotonic such that the vesicles assume spherical shape. Subsequently, we added appropriate volumes of a concentrated solution of a given solute to the starting suspension in order to bring the osmolarities of the same solute to those reported (see below) while maintaining the osmolarity of phosphate-buffered saline at 200 mosM. Usually 30 min was allowed for the ghost vesicles to reach the steady-state at a new osmolarity of any solute and the resulting ghost size was found to remain the same at least for 4–5 h. Although the ghost vesicle size determined in this way is quite insensitive to the vesicle concentration [8,9], we have maintained the vesicle concentration about the same within a factor of 2 at different carbohydrate osmolarities of the suspending medium.

As alluded to above, the size and shape of the vesicles are deduced from the scattering profile. This is effected by plotting $I_{vv}(\theta) \cdot \sin^2(\theta/2)$ against $\sin(\theta/2)$ and noting the extrema positions, where $I_{vv}(\theta)$ is the polarized scattering intensity at a scattering angle θ [11,12].

Quasielastic light scattering. Since the quasielastic light-scattering measurement is much more sensitive to the aggregation of the scattering particles, a fresh sample was made for each different osmolarity of solutions and filtered through a 10 μm Nucleopore filter once more. The experimental details are the same as previously reported [9]. And all light scattering measurements were done at room temperature (22 ± 1°C).

Results and Discussion

Ghost size. In Fig. 1 are displayed three typical profiles of elastic light scattering, with and without sucrose in the suspending medium. The top profile, without sucrose, represents the hypotonic limit at 200 mosM phosphate-buffered saline. The ghost size is determined from the profile with the spherical shell model whereby the position of each peak and valley of the modulation gives rise to a particular radius value and a set of these values is averaged to delineate the ghost radius in a given suspending medium. The radius thus determined at the hypotonic limit is 2.25 μm. This is the size that bovine ghosts attain as the maximum, which remains more or less stable before the ghosts eventually lyse upon further lowering of the osmolarity of suspending medium. We should also note that this maximum size is the same as the value of 2.22 ± 0.03 μm obtained for the ghosts prepared by the method of Dodge et al. [5] and suspended in a 20 mosM medium; this is known to produce partially sealed, hence osmotically unresponsive ghosts. The bottom two profiles of Fig. 1 make it apparent that the extrema shift to larger scattering angles as the sucrose osmolarity is increased, indicating that the ghosts become smaller.

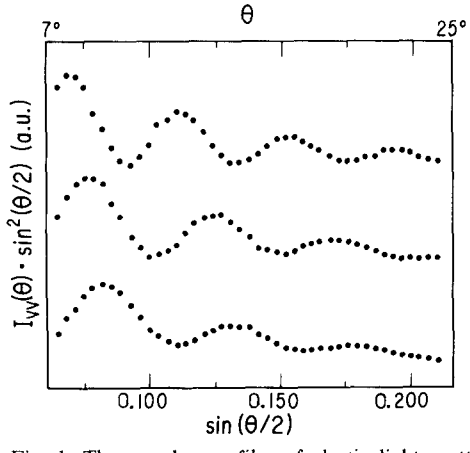

Fig. 1. The angular profiles of elastic light scattering of red blood cell ghosts in a hypotonic medium, 200 mosM phosphate-buffered saline (upper graph), and with added sucrose (+20 mosM sucrose, middle; +36 mosM, bottom graph). The incident radiation was 514.5 nm line of an argon ion laser, and the scattering was performed in the angle range 7–24.6° in 0.2°-increments.

The ghost vesicles, however, vary in size slightly with different blood samples, preparation lots and the preservation period after each ghost preparation. In order to compare the ghost size in different suspending media, these initial variations in size need to be taken into account; we characterize the size at any other conditions relative to that at the hypotonic limit as the reference. The size variation, however, rarely exceeds the precision of individual determinations, namely 1 S.D. (usually less than 3%), so that we rescale the size measurements relative to the common reference at 2.25 μm. Progression of the ghost size as a function of the suspending medium osmolarity is then expressed in terms of this reference size. We assume for the

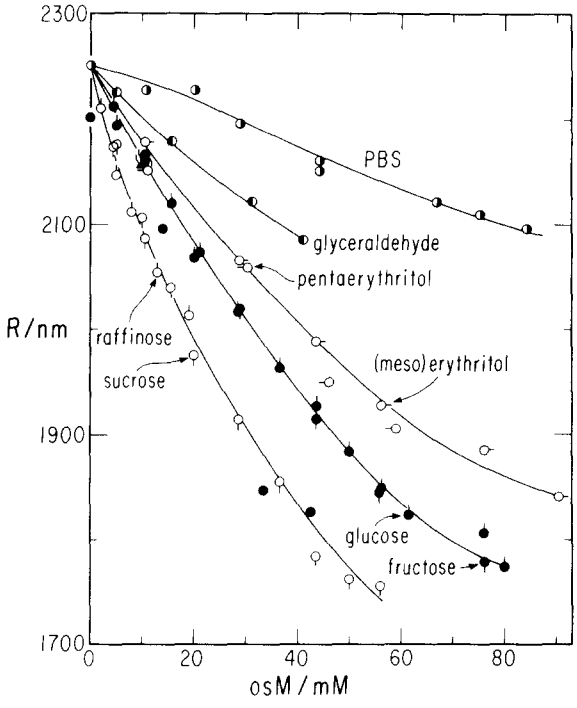

Fig. 2. The osmotic deformation profiles of red blood cell ghosts induced by different carbohydrates and phosphate-buffered saline added to the 200 mosM phosphate-buffered saline suspension. The ghost radius, R, is deduced from the elastic light-scattering profiles as shown in Fig. 1 according to the spherical shell model and the osmolarity of added sugars and phosphate-buffered saline is given in units of mM. In the bottom profile, where the data for raffinose and sucrose are shown, the Stokes radius determined by quasielastic light scattering as a function of added sucrose osmolarity is also plotted by filled circles.

moment that the ghost vesicles remain spherical in shape, hence the size is given in terms of the spherical shell radius. We shall shortly return to the issue of ghost shape. Now we are ready to discuss the osmotic deformation behavior.

Fig. 2 shows the deformation profiles for different test solutes. The ghosts are initially swollen in 200 mosM phosphate-buffered saline, and the size is plotted against the additional osmolarity of the test solutes. Raffinose and sucrose are almost indistinguishable, and they are clearly the most effective in producing osmotic deformation, from which we infer that the ghost membranes are practically impermeable to these two solutes. Furthermore, the membrane impermeability to sucrose with the resealed ghosts has been tested by measuring the release of entrapped [^{14}C]sucrose for ghosts prepared by several different procedures [13]. In this event, the deformation profile produced by these two sugars represents the maximum osmotic response of ghost vesicles since the larger sugar (raffinose) induces about the same extent of osmotic response as does sucrose, hence no other polysaccharide is expected to more efficacious in inducing osmotic deformation. Next, we examine the hydrolysis products of sucrose, glucose and fructose; they are almost identical in their effect on the ghosts, being osmotically less active than sucrose. Pentaerythritol and *meso*-erythritol, branched and linear tetrols, respectively, are even less effective in producing the osmotic deformation. As with the previous pair of isomers, they are identical in producing an osmotic gradient across the red blood cell ghost membrane. The smallest sugar analog tested, glyceraldehyde, falls between those of tetrols and sodium chloride, the principal components of phosphate-buffered saline which turns out to be the least effective species in generating the osmotic deformation among the solutes we have tested. Thus, the efficacy in producing the osmotic deformation can be ranked as phosphate-buffered saline < glyceraldehyde < pentaerythritol ≈ *meso*-erythritol < fructose < sucrose ≈ raffinose.

TABLE I

REVERSIBILITY TEST OF GHOST RADIUS IN DIFFERENT SUSPENDING MEDIA

The three different ghost samples employed are distinguished by A, B and C.

Measurement No.	Ghost sample	Osmolarity (mosM)	Radius (μm)
1	A	320	2.06 ± 0.03
2	A	470	1.86 ± 0.03
3	A	400	1.97 ± 0.04
4	A	320	2.06 ± 0.04
5	B	280	2.13 ± 0.04
6	B	240	2.20 ± 0.03
7	B	320	2.05 ± 0.04
8	C	170	2.25 ± 0.04

It should be noted parenthetically that the ghost vesicle size, as determined by elastic light scattering, is shown to be completely reversible and time-independent, at least up to 4–5 h, beyond which the scattering profile gradually deteriorates, presumably due to the degradation of membrane structure. The reversibility is documented as follows. The measured ghost size is shown to depend only on the osmolarity of suspending medium and is independent of the path by which a given size has come to be through different osmolarity media. Such is shown in Table I, where the ghost radius measurements in phosphate-buffered saline are collected in different sequences of the osmolarity change for the range 170–470 mosM; the measurement numbers 1–4 are the hypertonic branch and 5–8 are the hypotonic branch. From one measurement to the next, we allowed about 30 min for the ghosts to attain the new steady-state radius and three separate ghost samples, designated A, B and C, were used for this study. We find quite clearly the hypotonic branch reproduces the results shown in the uppermost part of Fig. 2.

Ghost shape. We now return to the issue of ghost shape during the osmotic deformation. Since the modulation profile of elastic light scattering is most sensitive to the semi-major axis dimension of ellipsoidal shells, e.g., oblate or prolate shells [10,11], it is not possible to extract the shape of scattering particles from the plot such as shown in Fig. 1; we can at best extract the semi-major axis dimension upon postulating a given shape of the scatterer. Thus, we need another experimental method in order to define the shape. The quasi-elastic light-scattering method is precisely such a method. The scheme of combining the two light-scattering methods to characterize the membrane vesicles in terms of their shape and size is now well

documented [10]. We have performed quasielastic light scattering to monitor the osmotic deformation with sucrose as the test solute. The homodyne autocorrelation technique was used [14]. A typical, normalized second-order autocorrelation function, $g^{(2)}(\tau)$, is shown in Fig. 3 where the solid curve is drawn by fitting the data to a single exponential decay profile:

$$g^{(2)}(\tau) = Ae^{-2\Gamma_1\tau} + B \qquad (1)$$

where A, B and Γ_1 are the three fitting parameters to be extracted. Sometimes it is necessary to eliminate the first 2–3 points out of 64 points which showed a faster decay, seemingly due to the

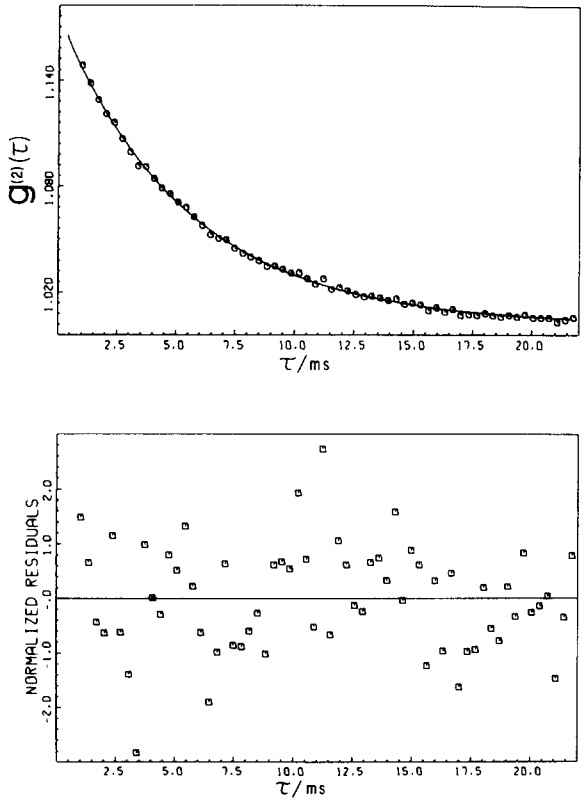

Fig. 3. An example of normalized second order autocorrelation function $g^{(2)}(\tau)$ is shown in the upper portion where $g^{(2)}(\tau)$ is plotted against time τ in units of ms, and the solid curve is the fitted single exponential decay according to Eqn. 1. In the bottom portion, the corresponding residuals plot is shown, where the ordinate is scaled in units of the standard deviation of residuals, $1.4 \cdot 10^{-3}$. The small magnitude coupled with the random pattern of the residuals indicate an excellent representation of the data by single exponential decay (Eqn. 1).

small fragments of the membrane. Contrary to the results of the ghosts prepared by the procedure of Dodge et al. [5], the three-parameter single-exponential analysis performed in this way is better than the double-exponential fit [15]. We also tried the second-order cumulant analysis [16]. From the bottom half of Fig. 3, we surmise that the single exponential, Eqn. 1, represents an excellent fit to the experimental data, as shown by a small standard deviation and random pattern of the residuals. From the decay constant Γ_1 of $g^{(2)}(\tau)$, we deduce the translational diffusion coefficient D through $\Gamma_1 = Dq^2$, where q is the scattering wave vector. After repeating the Γ_1 determination at several different scattering angles and confirming its q^2 dependence, we deduce the Stokes radius of the ghosts from D by use of the Stokes-Einstein equation. These Stokes radii are then compared with those obtained by elastic light scattering. This is shown in the bottom plot in Fig. 2 where the Stokes radii are given by filled circles. Within experimental uncertainty, the two sets of the ghost size are the same. We can, therefore, conclude that the ghost shape remains spherical up to about 40 mosM sucrose; otherwise, we should have observed different sets of the radii, and the Stokes radius should have been the smaller of the two for any symmetric deviation from the spherical shape. Since the deformation probed by the Stokes radius covers about the full range of the size variation and the nature of the deformation is presumed to be purely osmotic, it seems plausible to expect that what we observe with sucrose should prevail with other solutes. Under such circumstances, we reach the striking conclusion that spherical red blood cell ghosts at the hypotonic limit deform isotropically by the osmotic gradient across the membrane bilayer. In other words, the osmotic deformation of red blood cell ghosts takes place by isotropic contractions of the spherical shells.

Ghost volume and effective osmolarity. Displayed in Fig. 4 are such volume-contraction profiles. All the curves showed the expected sigmoidal decrease in volume. Having taken raffinose as the reference and shifting horizontally the other curves by a certain factor to the left to coincide with the raffinose profile, we obtain a single curve for all solutes as displayed in Fig. 5. The striking universality of the deformation profiles demonstrates

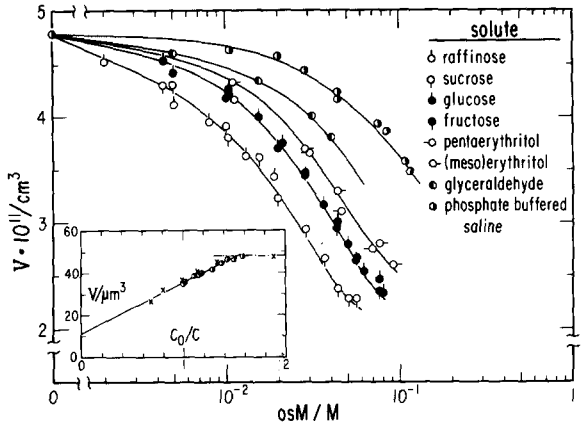

Fig. 4. The ghost volume calculated from R in Fig. 2 is plotted against the osmolarity of added carbohydrates and phosphate-buffered saline. The starting suspending medium was 200 mosM phosphate-buffered saline. In the inset, the ghost volume is plotted against the relative reciprocal osmolarity of phosphate-buffered saline, C_o/C, where C_o is the isotonicity, 320 mosM, and C is the total phosphate-buffered saline osmolarity at other states. The chained line at the right in the inset indicates the hypotonic limit of ghost volume, 48 μm^3.

that there exists a single factor which scales the osmotically effective concentration of each solute relative to the reference. These factors by which the test solutes are ranked relative to raffinose are listed in Fig. 5. Thus, the effective osmolarity toward the red blood cell membrane system is represented by the parameter, σ. For example, 1 mosM raffinose has the same effect as 3.6 mosM

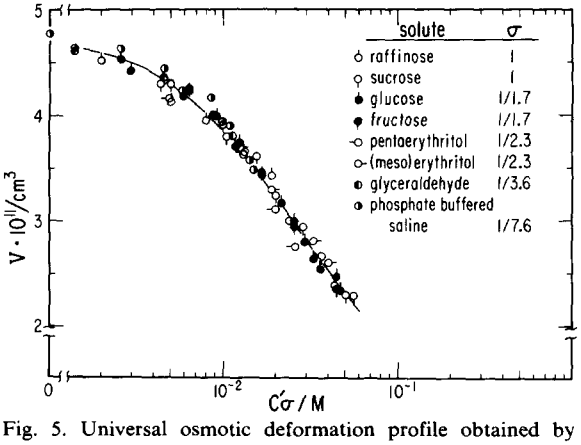

Fig. 5. Universal osmotic deformation profile obtained by rescaling the osmolarity of added sugars and phosphate-buffered saline, C', according to the effective osmolarity parameter, σ, relative to raffinose.

glyceraldehyde in inducing the osmotic contraction. In order to account for this behavior, the osmotic nonideality of the solute in question may need to be considered in computing the effective osmolarity. If we calculate the osmotic contributions due to the second virial term using the data of Kozak et al. [17], we find its contributions to be negligibly small. For example, 50 mM raffinose, which has the largest second virial coefficient among the carbohydrates tested, shows a contribution of no more than 2.5% over the Vant Hoff ideal osmolarity. Thus, we can conclude that the nonideal contribution to the osmotic pressure amounts to a small addition to the effective osmolarity; hence, we neglect these terms in expressing the solute osmolarity.

What is remarkable about the plot in Fig. 5 is that the parameter σ appears to be unique to a given size of sugar. Whether there indeed exists a simple correlation between the size of a sugar and its effective osmolarity remains to be examined in detail in the future. For now it suffices to note that our finding shown in Fig. 5 can be explained neither by the kinetic permeability concept [2] nor by the equilibrium osmosis model [18,19]. At the same time, it is crucial to note the distinction between our finding and the results of previous studies on red blood cell ghosts. In a given suspending medium, we find a well-defined spherical shape for the ghosts which does not change with time, at least up to 4–5 h, and reversible relative to changes in the osmolarity of suspending medium. Hence, we call the observed size parameter the steady-state quantity simply because we cannot confirm its time asymptotic value, presumably due to phospholipid oxidation and other chemical complications; otherwise, we would have called it the equilibrium quantity. In most of the previous studies, either the ghost volume is determined before the passive flux of a solute across the membrane bilayer has begun [20] or at some point after the flux starts but before the imposed osmotic gradient is essentially abolished by solute transport [6,21]. To the best of our knowledge, there exists no report of the steady-state volume of red blood cell ghosts as we are reporting here. The issue of time-dependence of ghost volume was first raised by Kwant and Seeman [20], but they did not note any steady-state volume; we infer from

their statements that once the ghost volume is established by water transport there follows subsequent volume changes due to passive solute transport. We will return to this point later. In addition, there is a clear difference in the experimental methods in deducing the volume. Our method relies on separate experiments to determine the vesicle radius and to confirm its spherical shape. On the other hand, a vast majority of the osmotic deformation studies to date depends on a cell-counting scheme, such as Coulter counter, to deduce the mean cell volume upon calibrating it against certain standards. Another common method is to determine the cell number density first by a separate method and measure the total cell volume with use of hematocrit tubes. It is, therefore, rather obvious that ours is a more direct and absolute method because it probes the scatterers (ghosts) in situ microscopically with visible wavelength and deduces the average size and shape in a given suspending medium without relying upon separate standardization procedures. It, however, is also restrictive to the extent that the features in the elastic scattering profiles can only be seen with a fairly narrow distribution of the ghost size. Had the distribution been broader, we could not have measured the radius with the same precision. The scattering methods by nature require that the scatterers remain stable during the measurements which take time to perform, about 30 min for elastic scattering and a few minutes for quasielastic scattering. Hence, our method is not appropriate for transient size determinations.

Nature of osmotic deformation. We conclude this report by pointing out the issues that our results raise relative to the references in the literature concerning the properties of red blood cell ghosts. Kwant and Seeman [20] concluded that human red blood cell ghosts behave like 'perfect osmometers' if the ghost volume in response to the imposed osmotic gradient is measured before any solute flux across the membrane takes place, in particular within 30–60 s. A perfect osmometer in their context means that (1) the membrane is strictly semipermeable, i.e., permeable only to water and impermeable to all solutes, and (2) it poses no resistance to contraction or expansion such that osmotically active ghost volume V_a adjusts to equalize the interior osmolarity to the exterior one, that of the suspending medium, C. If so, they argue, V_aC should be constant for the entire range of C at a given temperature, and the constant can be determined through a chosen reference state, such as the hypotonic hemolysis condition. It follows that the total ghost volume V, which exceeds V_a by a small cell volume V_c, should be proportional to C^{-1}. This is the behavior of ghost volume changes they have observed, and from this they claim that the 'perfect osmometer' behavior is established. We now offer our critique of this claim. In so doing, we will avoid any reference to the quality of ghost preparations, which appears to have improved greatly since 1970 [4]. According to their model, the ghost volume change arises entirely from the water transport across the membrane bilayer. Once a requisite amount of water is effluxed or influxed to equalize the osmolarity across bilayer, the equilibrium should now be established and no more water transport must take place until another osmotic gradient is imposed. If the same solute as in the hemolysis medium, e.g., NaCl, is used to impose the osmolarity gradient, then the ghost volume should remain the same even if the membrane is permeable to the constituent ions because the driving chemical potential gradients due to all permeable components are abolished at this point. Clearly this was not the case when Kwant and Seeman [20] had to measure the volume within 30–60 s. More recently, Jausel-Hüsken and Deuticke [13] have observed the ghost volume changes lasting as long as 4 h. Thus, it is not even clear whether the driving chemical potential of osmotic deformation is understood, let alone the quantitative behavior of a 'perfect osmometer'. Secondly, the perfect osmometer should pose no resistance to contraction of ghost volume, hence the hypertonic limit of ghost volume must be so small as to account for only the volume of membraneous materials, 1–2% of the total ghost volume according to Kwant and Seeman [20]. On the other hand, Weed et al. [6] found a substantial limiting volume at the extreme hypertonicity. Our finding with bovine red blood cell ghosts is in accord with the latter. This is shown in the inset of Fig. 4 where a plot of V vs. $1/C$ is displayed for phosphate-buffered saline, which is chosen because the same solute is used for hemolysis and suspending media for the osmolarity gradient. Here we call

attention to three distinct observations: (1) the total volume V is proportional to $1/C$; (2) the hypertonic limiting volume, V $(1/C \rightarrow 0)$, is as large as about 12–15 μm^3, amounting to 33–41% of the total isotonic volume; and (3) there is a well-defined hypotonic limiting volume, V $(1/C \rightarrow \infty)$, at 48 μm^3 (marked by the chained line), beyond which the ghost volume no longer expands but reaches the ultimate strength whereby ghosts burst on further lowering of the osmolarity. The limiting upper and lower volumes are suggestive of a finite resistance to deformation due to the membrane stiffness, and in such an event the linear dependence of V on $1/C$ seems hardly a necessary condition for the perfect osmometer behavior. A number of recent studies on the elastic continuum property of human red blood cell membrane suggests [22] that the equivalent three-dimensional modulus is of the order of 10^4 dyn/cm^2, which is scarcely a negligible quantity, and a material with such a magnitude of modulus cannot possibly be regarded as having no resistance to deformation. Taking these discordant results together, we feel compel to propose that a systematic study of the steady-state behavior must be undertaken. Why such behavior of the red blood cell ghosts of any mammalian origin has not been reported is a great mystery to us. Our immediate task is to effect a similar set of measurements with human red blood cell ghosts. This will be the subject of our next report.

Acknowledgements

This work is in part supported by an NIH grant, EY01483, and grants from the Knapp Scholarship Fund to P.B.S. and the Trewartha Honors Undergraduate Research Fund to D.A.D. We thank Messrs. Terry N. Timm and James V. Lochner of the Muscle Biology laboratory of the University for their help in obtaining fresh cow blood.

References

1 Surgenor, D.M. (ed.) (1975) The Red Blood Cell, Academic Press, New York
2 Ellory, J.C. and Lew, V.L. (eds.) (1977) Membrane Transport in Red Cells, Academic Press, New York
3 Steck, T.L. (1974) in Methods in Membrane Biology (Korn, E.D., ed.) pp. 245–281, Plenum Press, New York
4 Steck, T.L. and Kant, J.A. (1974) Methods Enzymol. 31, 172–180
5 Dodge, J.T., Mitchell, C. and Hanahan, D.J. (1963) Arch. Biochem. Biophys. 100, 119–130
6 Weed, R.I., Reed, C.F. and Berg, G. (1963) J. Clin. Invest. 42, 581–588
7 Jung, C.Y. (1971) Arch. Biochem. Biophys. 146, 215–226
8 Amis, E.J., Wendt, D.J., Erickson, E.D. and Yu, H. (1981) Biochim. Biophys. Acta 664, 201–210
9 Amis, E.J. (1981) Ph.D. Thesis, University of Wisconsin
10 Yu, H. (1982) Methods Enzymol. 81, 616–629
11 Norisuye, T. and Yu, H. (1977) Biochim. Biophys. Acta 471, 436–452
12 Yu, H. (1981) J. Res. Nat. Bur. Stand. 86, 571–590
13 Jansel-Hüsken, S. and Deuticke, B. (1981) J. Membr. Biol. 63, 61–70
14 Bern, B.J. and Pecora, R. (1976) Dynamic Light Scattering, Wiley-Interscience Publication, New York
15 Bargeron, C.B. (1973) Appl. Phys. Lett. 23, 379–381
16 Koppel, D.E. (1972) J. Chem. Phys. 57, 4814–4820
17 Kozak, J.J., Knight, W.S. and Kauzmann, W. (1968) J. Chem. Phys. 48, 675–690
18 Jacobs, M.H. and Stewart, D.R. (1947) J. Cell. Comp. Physiol. 30, 79–103
19 Dick, D.A.T. (1965) Cell Water, Butterworth Inc., Washington
20 Kwant, W.O., and Seeman, P. (1970) J. Gen. Physiol. 55, 208–219
21 Teorell, T. (1952) J. Gen. Physiol. 35, 669–701
22 Hochmuth, R.M. (1982) Annu. Rev. Biophys. Bioeng. 11, 43–55